

¹ 3DQLayers: Volumetric Layer Based Analysis for Quantitative Renal MRI

³ Alexander J Daniel  ^{1,¶} and Susan T Francis  ^{1,2}

⁴ 1 Sir Peter Mansfield Imaging Centre, University of Nottingham, Nottingham, United Kingdom 2 NIHR
⁵ Nottingham Biomedical Research Centre, Nottingham University Hospitals NHS Trust and the University
⁶ of Nottingham, Nottingham, United Kingdom ¶ Corresponding author

DOI: [10.xxxxxx/draft](https://doi.org/10.xxxxxx/draft)

Software

- [Review](#) 
- [Repository](#) 
- [Archive](#) 

Editor: [Open Journals](#) 

Reviewers:

- [@openjournals](#)

Submitted: 01 January 1970

Published: unpublished

License

Authors of papers retain copyright and release the work under a Creative Commons Attribution 4.0 International License ([CC BY 4.0](#)).

⁷ Summary

⁸ Quantitative Magnetic Resonance Imaging (qMRI) provides informative measurements of the
⁹ structure and function of an organ where each volumetric pixel (voxel) provides a measure of the
¹⁰ physical properties of the underlying tissue. Traditionally, analysis of MR images is performed
¹¹ by first segmenting the organ and its constituent tissue types, which for the kidneys involves
¹² separating them into the cortex and medulla, before calculating the average measurement
¹³ within each tissue. The process of segmenting renal tissue types is typically manual, making it
¹⁴ time consuming and prone to inaccuracies.

¹⁵ An alternative to voxel-based analysis in MRI is the layer model which divides the organ into
¹⁶ ordered surfaces. For the kidney, this involves generating layers based on the distance of each
¹⁷ voxel between the outer and inner surface of the kidney. From this, the gradient of change in
¹⁸ qMRI measures between the cortex and medulla of the kidney can be computed to evaluate
¹⁹ pathological and physiological aspects of the kidney. Here, 3DQLayers, an open-source Python
²⁰ software package to automatically define and interrogate 3D renal layers is presented.

²¹ Statement of need

²² Background

²³ The kidneys are structurally and functionally complex organs in the abdomen responsible for
²⁴ the removal of waste products and excess fluid from the blood to produce urine ([Lote, 2012](#)).
²⁵ Each kidney is separated into the cortex which forms the outer layer of the kidney and the
²⁶ medulla in the inner part which is arranged in a series of small pyramids ([Hall, 2015](#)), as shown
²⁷ in [Figure 1](#). The kidney maintains homeostasis through filtration, reabsorption, secretion, and
²⁸ maintenance of the cortico-medullary gradient (CMG), meaning a method to assess changes in
²⁹ physiology from the cortex to the medulla is key.

³⁰ Conventional MRI primarily assesses signal intensity in a voxel in arbitrary units, however
³¹ Quantitative MRI (qMRI) goes beyond conventional MRI by instead providing voxel-wise
³² measurements with numerical significance in physical units, based on the tissues underlying
³³ properties. For example, qMRI of relaxation times with parameters which carry information
³⁴ about the local microstructure, or those of how readily water can diffuse through the tissue,
³⁵ and the rate at which blood perfuses the tissue. To interpret quantitative images, regions of
³⁶ interest (ROIs) for the kidney cortex and medulla are defined and statistical analysis performed
³⁷ on the voxels within each ROI. Segmenting such ROIs manually is time consuming, and prone
³⁸ to intra- and inter-reader variation.

³⁹ The group of Pruijm proposed an alternative to voxel based ROI analysis of tissue termed
⁴⁰ the Twelve Layer Concentric Object (TLCO) method ([Li et al., 2020](#); [Milani et al., 2017](#);

⁴¹ Piskunowicz et al., 2015) where users delineate the inner and outer boundaries of the kidney
⁴² to generate twelve equidistant layers between the renal pelvis and the surface of the kidney.
⁴³ The outer layers represent the cortex and the inner layers the medulla, with the gradient across
⁴⁴ the central layers computed to estimate the CMG. Since this layer-based analysis only requires
⁴⁵ segmentation of the boundaries of the kidney, rather than the cortex and medulla within, it
⁴⁶ is quicker and more repeatable. An analogy to this is the development of the layer-based
⁴⁷ analysis tools applied in the brain for neuroimaging including BrainVoyager (Goebel, 2012),
⁴⁸ CBSTools/Nighres (Bazin et al., 2014; J. Huntenburg et al., 2017; J. M. Huntenburg et al.,
⁴⁹ 2018), FreeSurfer (Fischl, 2012), and FSL (Jenkinson et al., 2012).

⁵⁰ However, the TLCO software is closed-source and has some limitations. It requires manual
⁵¹ delineation of the outside and inside surfaces of the kidney, divides the kidney into the same
⁵² number of layers irrespective of the size of the kidney, and can only be performed on a single
⁵³ slice cutting through the kidneys on their longest axis (coronal-oblique) which is not always
⁵⁴ desirable (Bane et al., 2020). Due to the spatial distribution of kidney pathology, there is a
⁵⁵ need to acquire multi-slice images for full 3D coverage of the kidney to increase the number of
⁵⁶ voxels sampled and gain a better understanding of the heterogeneity of the kidney. Recently,
⁵⁷ an automated-TLCO method has been proposed (Ishikawa et al., 2022) to determine the CMG
⁵⁸ from the water signal of a Dixon scan, however this work again has limitations of not being
⁵⁹ full kidney coverage, including the renal pelvis, and highlights the difficulty in analysing small
⁶⁰ kidneys with a fixed number of layers.

⁶¹ The motivation of 3DQLayers was to address these limitations of TLCO to provide an open-
⁶² source Python package to automatically define 3D, multi-slice layers in the kidney of known
⁶³ thickness for quantitative-depth based analysis across a range of kidney MRI data, enabling its
⁶⁴ use in large renal MRI trials to address clinical questions.

⁶⁵ Methods

⁶⁶ 3DQLayers is an open-source Python package building on the ideas within TLCO, with the
⁶⁷ fundamental difference that the layers are defined based on a voxels' distance from the surface
⁶⁸ of the kidney in millimetres rather than the proportion of the kidney. As such, the input to
⁶⁹ 3DQLayers is a whole kidney mask, which can be automatically generated from a structural
⁷⁰ image e.g. here using a U-net applied to T₂-weighted images (Daniel et al., 2021; Daniel,
⁷¹ 2024).

⁷² The pipeline for defining the layers from the whole kidney mask is outlined in Figure 2. Pre-
⁷³ processing steps first fill in the holes in the kidney mask caused by cysts, as the surface of a
⁷⁴ cyst is not characteristic of the surface of the kidney. Next, the voxel-based representation of
⁷⁵ the mask is converted to a smoothed mesh-based representation of the kidneys, the distance
⁷⁶ from the centre of each voxel to the surface of the mesh is calculated to produce a depth
⁷⁷ map (Dawson-Haggerty, 2023). Tissue adjacent to the renal pelvis that is not representative
⁷⁸ of the medulla is then excluded from layer-based analysis. This is achieved by automatically
⁷⁹ segmenting the renal pelvis then calculating the distance from each voxel to the renal pelvis as
⁸⁰ described above. Those voxels closer than a specified threshold, typically 10 mm, are excluded
⁸¹ from the depth map. Finally, a layer image is generated by quantising the depth map to a
⁸² desired layer thickness, typically 1 mm.

⁸³ The layer image and quantitative images are resampled to the same spatial resolution using
⁸⁴ NiBabel (Brett et al., 2023), to allow each layer to be used as an ROI to interrogate each
⁸⁵ qMRI image with statistical measures (e.g. median, standard deviation and kurtosis) across
⁸⁶ the depth of the kidney. The gradient of the central layers can be calculated to estimate the
⁸⁷ CMG in qMRI metrics. These metrics can be computed for the left and right kidney separately,
⁸⁸ or analysed in a combined manner. Additionally, if the renal cortex and medulla ROIs are
⁸⁹ available, the distribution of tissue types across layer depth can be explored and an estimate
⁹⁰ of average cortical thickness calculated. As the layers are generated from a structural image
⁹¹ rather than the quantitative map, using 3DQLayers stipulates no requirements on quantitative

92 map acquisition, unlike TLCO.

93 An object-oriented interface is provided to allow end users to simply generate layers and apply
94 these to qMR images. Documentation is provided to guide users through installation via PyPI,
95 conda or from source code on GitHub; it also includes tutorials and an API reference. An
96 automated test suite with high coverage provides users with confidence in the stability of
97 3DQLayers and that there will be no unexpected changes to results unless highlighted in the
98 change-log.

99 Usage Examples

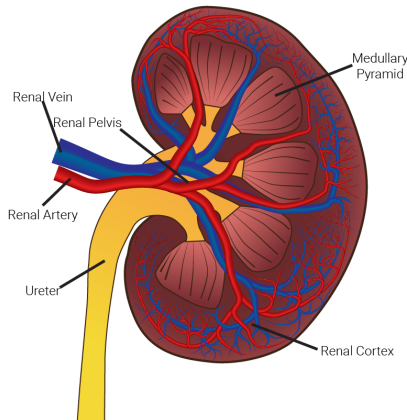
100 Figure 3 shows the application of 3DQLayers to measure different gradients of the transverse
101 relaxation rate R_2^* in a healthy volunteer with normal renal function and a patient with impaired
102 renal function (an estimated glomerular filtration rate (eGFR) of above 90 ml/min/1.73m²
103 measured from blood samples is considered in the healthy range (Stevens et al., 2006)).
104 This replicates results shown using TLCO, with a lower gradient in patients compared to
105 healthies, however 3DQLayers controls for kidney size resulting in the gradient being measured in
106 quantitative units of Hz/mm rather than Hz/layer as in TLCO, thus increasing generalisability.

107 Figure 4 shows how 3DQLayers can be used in combination with cortex and medulla tissue ROIs
108 to analyse the distribution of voxel counts of each tissue as a function of layer depth of the
109 kidney. Here cortex and medulla ROIs are initially generated using a Gaussian mixture model to
110 segment a T₁-weighted structural image followed by manual ROI correction. From this, average
111 renal cortical thickness can be defined from the depth at which the voxel distribution crosses
112 from cortex to medulla. Cortical thickness has been hypothesised as a potential biomarker of
113 renal disease (Korkmaz et al., 2017; Yamashita et al., 2015).

114 3DQLayers can also be used to analyse ex-vivo kidneys imaged outside the body. Figure 5 shows
115 example quantitative maps acquired from a kidney retrieved for transplant but subsequently
116 deemed unsuitable and the associated layer profiles. Figure 6 compares the results of tissue ROI
117 based analysis and layer-based analysis in fifteen transplant kidneys. A significant correlation
118 between outer layers and the cortex, and inner layers and the medulla was shown across all
119 quantitative mapping techniques and a significant correlation between cortico-medullary ratio
120 and layer gradient was shown for T₁, T₂, T₂^{*} and Magnetisation Transfer Ratio (MTR)
121 mapping.

122 **Figures**

a.



b.

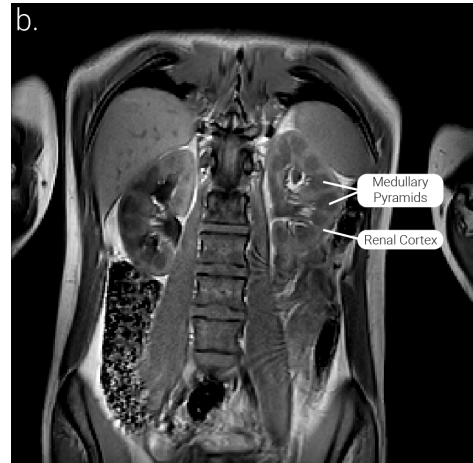


Figure 1: a) A schematic of the kidneys showing the renal cortex and medullary pyramids. b) A T₁-weighted structural MR image of the abdomen showing the kidneys with the renal cortex appearing as a light band on the outer edge of the kidney and the medullary pyramids as darker patches on the inner portion of the kidneys.

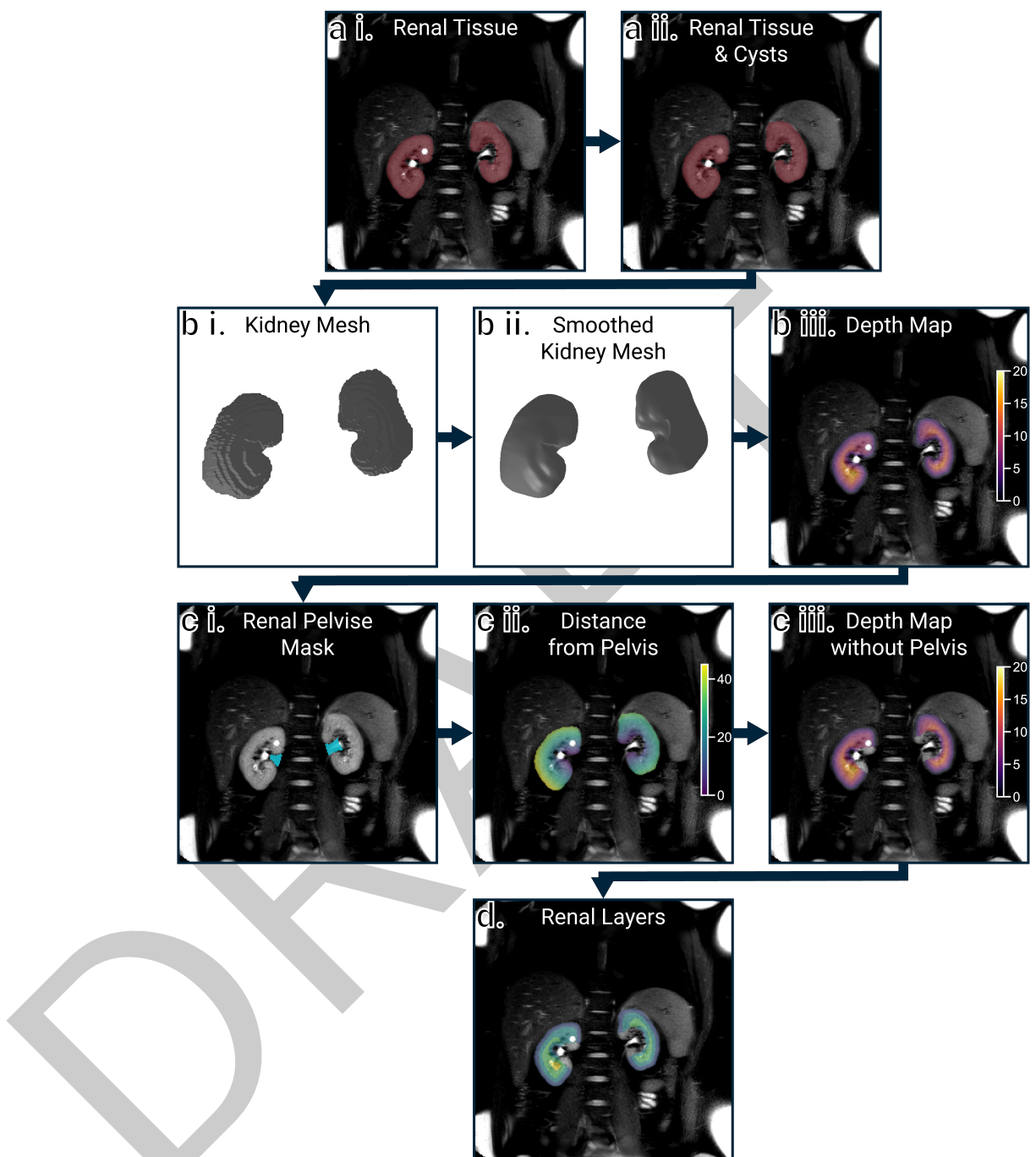


Figure 2: The mask automatically computed using a U-net from the T₂-weighted structural MR image (a i) has any cysts filled (a ii) and is converted into a smooth mesh representing the renal surface (b i and ii). The distance (in mm) of each voxel to the surface of the mesh is then calculated to generate a depth map (b iii). The renal pelvis is segmented (c i) and any tissue within 10 mm (c ii) of the pelvis is excluded from the depth map (c iii). The tissue is then grouped into layers of a desired thickness, here shown as 5 mm renal layers for illustrative purposes (d).

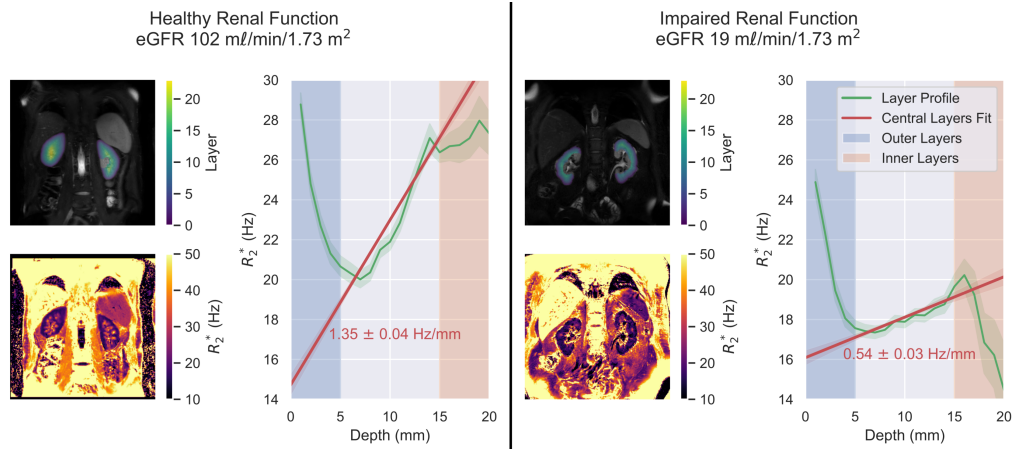


Figure 3: Layers, R_2^* maps, layer profiles, and central layer gradients for the left and right kidneys combined measured using 3DQLayers. Examples are shown for a subject with normal renal function and a patient with impaired renal function. Shading around profiles shows the 95% confidence interval within each layer.

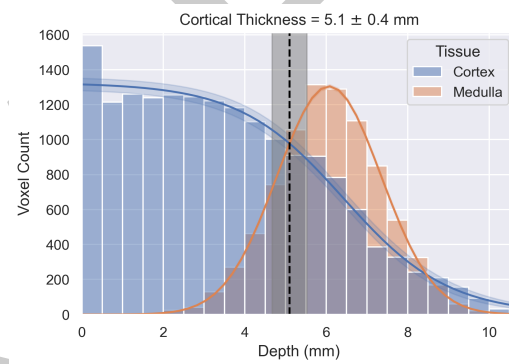


Figure 4: Exploring the distribution of tissue types through the kidney to measure cortical thickness.

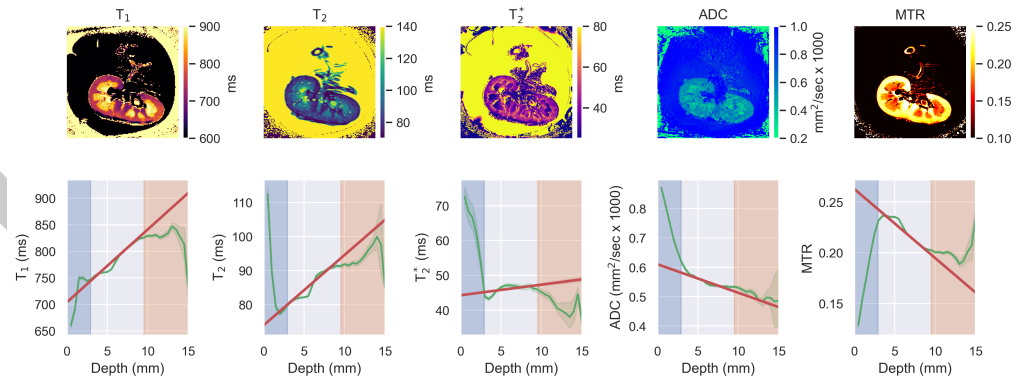


Figure 5: Example quantitative maps and associated layer profiles when 3DQLayers is applied to ex-vivo transplant kidneys. Uncertainty shading shows the 95% confidence interval of each layer.

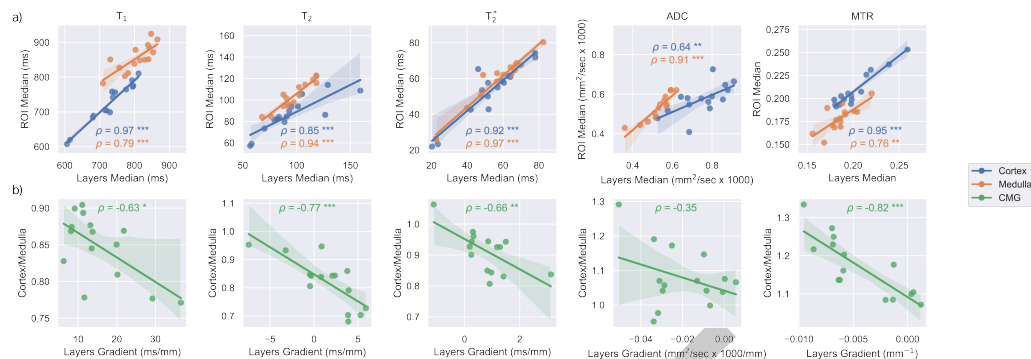


Figure 6: Agreement between tissue ROI-based measures and analogous layer-based measures shown for fifteen ex-vivo transplant kidneys for each qMRI alongside the Pearson's correlation coefficient (ρ). * represents a p -value between 0.05 and 0.01, ** between 0.01 and 0.001, and *** < 0.001 . a) Plots the median within each tissue ROI (cortex or medulla semi-automatically defined) against the equivalent layers (outer layers and inner layers respectively as highlighted in Figure 5) b) Shows the cortico-medullary ratio (calculated by dividing the median within the cortex ROI by the median within the medullary ROI) against central layer gradient profiles calculated using 3DQLayers.

123 Acknowledgements

124 We acknowledge the funding support of the ADMIRE project funded through Kidney Research
 125 UK (KS_RP_002_20210111), and the UKRIN_MAPS project funded by the Medical Research
 126 Council (MR/R02264X/1), as well as the NIHR Nottingham Biomedical Research Centre during
 127 the genesis of this project.

128 References

- 129 Bane, O., Mendichovszky, I. A., Milani, B., Dekkers, I. A., Deux, J.-F., Eckerbom, P., Grenier,
 130 N., Hall, M. E., Inoue, T., Laustsen, C., Lerman, L. O., Liu, C., Morrell, G., Pedersen,
 131 M., Pruijm, M., Sadowski, E. A., Seeliger, E., Sharma, K., Thoeny, H., ... Prasad, P. V.
 132 (2020). Consensus-based technical recommendations for clinical translation of renal BOLD
 133 MRI. *Magnetic Resonance Materials in Physics, Biology and Medicine*, 33(1), 199–215.
<https://doi.org/10.1007/s10334-019-00802-x>
- 134 Bazin, P.-L., Weiss, M., Dinse, J., Schäfer, A., Trampel, R., & Turner, R. (2014). A
 135 computational framework for ultra-high resolution cortical segmentation at 7 Tesla. *NeuroImage*, 93, 201–209. <https://doi.org/10.1016/j.neuroimage.2013.03.077>
- 136 Brett, M., Markiewicz, C. J., Hanke, M., Côté, M.-A., Cipollini, B., McCarthy, P., Cheng, C.
 137 P., Halchenko, Y. O., Cottaar, M., Ghosh, S., Larson, E., Wassermann, D., Gerhard, S.,
 138 Lee, G. R., Kastman, E., Rokem, A., Madison, C., Morency, F. C., Moloney, B., ... freec84.
 139 (2023). *NiBabel* (Version 5.1.0). Zenodo. <https://doi.org/10.5281/zenodo.591597>
- 140 Daniel, A. J. (2024). *Renal Segmentor* (Version 1.3.9). <https://doi.org/10.5281/zenodo.4068850>
- 141 Daniel, A. J., Buchanan, C. E., Allcock, T., Scerri, D., Cox, E. F., Prestwich, B. L., & Francis,
 142 S. T. (2021). Automated renal segmentation in healthy and chronic kidney disease subjects
 143 using a convolutional neural network. *Magnetic Resonance in Medicine*, 86(2), 1125–1136.
<https://doi.org/10.1002/mrm.28768>
- 144 Dawson-Haggerty, M. (2023). *Trimesh* (Version 4.0.0). <https://github.com/mikedh/trimesh>
- 145 Fischl, B. (2012). FreeSurfer. *NeuroImage*, 62(2), 774–781. <https://doi.org/10.1016/j.neuroimage.2012.01.021>

- 151 Goebel, R. (2012). BrainVoyager — Past, present, future. *NeuroImage*, 62(2), 748–756.
152 <https://doi.org/10.1016/j.neuroimage.2012.01.083>
- 153 Hall, J. E. (2015). *Guyton and Hall Textbook of Medical Physiology*. Elsevier Health Sciences.
154 ISBN: 978-1-4557-7005-2
- 155 Huntenburg, J. M., Steele, C. J., & Bazin, P.-L. (2018). Nighres: Processing tools for high-
156 resolution neuroimaging. *GigaScience*, 7(7), giy082. <https://doi.org/10.1093/gigascience/giy082>
157
- 158 Huntenburg, J., Wagstyl, K., Steele, C., Funck, T., Bethlehem, R., Fouquet, O., Larrat, B.,
159 Borrell, V., & Bazin, P.-L. (2017). Laminar Python: Tools for cortical depth-resolved
160 analysis of high-resolution brain imaging data in Python. *Research Ideas and Outcomes*, 3,
161 e12346. <https://doi.org/10.3897/rio.3.e12346>
- 162 Ishikawa, M., Inoue, T., Kozawa, E., Okada, H., & Kobayashi, N. (2022). Framework for
163 estimating renal function using magnetic resonance imaging. *Journal of Medical Imaging*,
164 9(2), 024501. <https://doi.org/10.1117/1.JMI.9.2.024501>
- 165 Jenkinson, M., Beckmann, C. F., Behrens, T. E. J., Woolrich, M. W., & Smith, S. M. (2012).
166 FSL. *NeuroImage*, 62(2), 782–790. <https://doi.org/10.1016/j.neuroimage.2011.09.015>
- 167 Korkmaz, M., Aras, B., Güneyli, S., & Yılmaz, M. (2017). Clinical significance of renal
168 cortical thickness in patients with chronic kidney disease. *Ultrasonography*, 37(1), 50.
169 <https://doi.org/10.14366/usg.17012>
- 170 Li, L.-P., Milani, B., Pruijm, M., Kohn, O., Sprague, S., Hack, B., & Prasad, P. (2020). Renal
171 BOLD MRI in patients with chronic kidney disease: Comparison of the semi-automated
172 twelve layer concentric objects (TLCO) and manual ROI methods. *Magnetic Resonance
173 Materials in Physics, Biology and Medicine*, 33(1), 113–120. <https://doi.org/10.1007/s10334-019-00808-5>
174
- 175 Lote, C. J. (2012). *Principles of Renal Physiology*. Springer Science & Business Media.
176 ISBN: 978-94-011-4086-7
- 177 Milani, B., Ansaloni, A., Sousa-Guimaraes, S., Vakilzadeh, N., Piskunowicz, M., Vogt, B.,
178 Stuber, M., Burnier, M., & Pruijm, M. (2017). Reduction of cortical oxygenation in
179 chronic kidney disease: Evidence obtained with a new analysis method of blood oxygenation
180 level-dependent magnetic resonance imaging. *Nephrology Dialysis Transplantation*, 32(12),
181 2097–2105. <https://doi.org/10.1093/ndt/gfw362>
- 182 Piskunowicz, M., Hofmann, L., Zuercher, E., Bassi, I., Milani, B., Stuber, M., Narkiewicz, K.,
183 Vogt, B., Burnier, M., & Pruijm, M. (2015). A new technique with high reproducibility
184 to estimate renal oxygenation using BOLD-MRI in chronic kidney disease. *Magnetic
185 Resonance Imaging*, 33(3), 253–261. <https://doi.org/10.1016/j.mri.2014.12.002>
- 186 Stevens, L. A., Coresh, J., Greene, T., & Levey, A. S. (2006). Assessing Kidney Function —
187 Measured and Estimated Glomerular Filtration Rate. *New England Journal of Medicine*,
188 354(23), 2473–2483. <https://doi.org/10.1056/NEJMra054415>
- 189 Yamashita, S. R., Atzingen, A. C. von, Iared, W., Bezerra, A. S. de A., Ammirati, A. L.,
190 Canziani, M. E. F., & D'Ippolito, G. (2015). Value of renal cortical thickness as a predictor
191 of renal function impairment in chronic renal disease patients. *Radiologia Brasileira*, 48(1),
192 12. <https://doi.org/10.1590/0100-3984.2014.0008>